Regular Article

PHYSICAL CHEMISTRY RESEARCH
Published by the
Iranian Chemical Society
www.physchemres.org
info@physchemres.org

Phys. Chem. Res., Vol. 9, No. 3, 483-507, September 2021
DOI: 10.22036/pcr.2021.261506.1865

Functionalized Banana Stalk for Lumefantrine Drug Removal

O.S. Agboola[a], S.B. Akanji[a] and O.S. Bello[a,b,*]

[a]*Department of Pure and Applied Chemistry, Ladoke Akintola University of Technology, P.M.B. 4000, Ogbomoso, Oyo State, Nigeria*
[b]*Department of Physical Sciences, Industrial Chemistry Programme, Landmark University, Omu-Aran, Nigeria*

(Received 11 December 2020, Accepted 13 March 2021)

Functionalized banana stalk (BSAC) was investigated as a potential adsorbent in removing a commonly used pharmaceutical antimalaria drug, Lumefantrine (LUMF). The raw banana stalk was chemically treated with orthophosphoric acid to enhance its adsorptive properties. The effect of LUMF initial concentration, temperature, solution pH and contact time on the adsorption process was studied using the batch equilibrium process. The surface characteristics of the prepared adsorbent were investigated using SEM, FTIR, proximate analysis and the Boehm titration techniques. The FTIR spectra showed notable peaks that are responsible for the adsorptive uptake of LUMF. The micrograph from the SEM showed well-developed pores which can be attributed to the effect of the acid treatment, and results from the proximate analysis showed 73.92% carbon content which is a remarkable percentage for a favorable uptake. The Sips isotherm model best fitted the experimental data with an $R^2 = 1$, and a maximum adsorption capacity of 102.1 mg g^{-1}. The closeness of the n values obtained from the Sips isotherm to 1 makes the model approach that of the Langmuir isotherm suggesting a monolayer coverage of LUMF on the BSAC surface. The pseudo-second-order kinetic model best explains the kinetics of adsorption of LUMF onto BSAC with R^2 values ranging from 0.9845-0.9997. The optimum pH recorded for this study was found between 5-7, and the pH_{pzc} for the BSAC was obtained at 4.5. Parameters obtained from the thermodynamic studies suggest that LUMF uptake by BSAC is endothermic, spontaneous, and thermodynamically favored ($\Delta H° = +46.83$ kJ mol^{-1}, $\Delta S° = +0.242$ kJ K^{-1} mol^{-1} and $\Delta G° = -41.66$ kJ mol^{-1}). BSAC was found to be effective in removing LUMF from aqueous solutions.

Keywords: Lumefantrine, Banana stalk activated carbon, Adsorption, Kinetics, Isotherm

INTRODUCTION

Water remediation has become an indispensable step needed to be taken by both the developed and developing countries to restrict the incessant disruption of ecological safety caused by pollutants. The introduction of pollutants to water and water sources has posed a great threat to ecological system. One of the fast-increasing pollutants found in water bodies is the pharmaceuticals which are a sub-division of a group of pollutants referred to as Emerging Contaminants (E.C) [1,2]. The release of pharmaceutical effluent into water endangers the various life species in the ecology. Pharmaceuticals are readily bio-accumulated, persistent, and have low bio-degradation [3]. Due to the frequent use of these drugs both in humans and veterinary medicine, their presence in water bodies is becoming a serious concern as a result of the alarming consequences.

Two major sources account for the ubiquitous presence of these pollutants in portable water. The common usage of drugs in farm and urban wastewater is one source while the other is a result of pharmaceutical processes in the industry [4,5]. Commonly used pharmaceutical products are anti-inflammatory drugs, analgesics, antibiotics, anti-malaria, fertility pills, and others [3] causing pollution of both ground and surface waters [6,7]. Due to the surge in the presence of the pharmaceutical products in aqueous environments, many researchers have reviewed the occurrence of these contaminants in receiving water bodies [8-19]. As it is necessary to keep the ecological health in

*Corresponding author. E-mail: osbello06@gmail.com

good shape and to make available portable and safe water, it is also important to develop methods to treat pharmaceutical contaminated waters before they are discharged into the environment [20,21]. Unfortunately, conventional methods have proven not sufficient for the treatment of wastewater; therefore, it is imperative to develop methods that will efficiently remove these pharmaceuticals from water sources.

Consequently, adsorption process provides an uncomplicated operational mode and design to completely remove pollutants, without generating unfriendly by-products in its operation [4,22]. This treatment method is shown to be efficient for the removal of pharmaceuticals and their residues from wastewater effluents [23,24]. The most widely used adsorbent is activated carbon due to its effectiveness in removing pollutants. The commercially prepared activated carbon comes with a high cost. Therefore, it is imperative to prepare an alternative, cheap, and readily available activated carbon, particularly from agricultural waste materials. Other adsorbent materials reportedly used for the sequestration of pollutants include Rice Husk, waste rubber tire, ZnO/Ag nanocomposite, mesoporous carbon, copper oxide nanoparticles, polyhydroquinone/graphene nanocomposite, Fe@Au core-shell, bagasse fly ash, Hg doped ZnO nanorods, ZnO/CuO nanocomposite, multi-walled carbon nanotubes, tire derived carbons, fullerenes, carbon nanotubes, porous carbon, slag, ZnO-NR-AC, and starch/PVA composite films [25-65]. In this study, banana stalk from agricultural waste was used to effectively remove Lumefantrine, an anti-malaria drug from polluted water. The cost-effectiveness associated with producing the improved activated carbon from banana stalk coupled with the high partition coefficient (PC) obtained in this study for the sequestration of LUMF could be novelty for this work. To the best of our knowledge, no studies have been conducted on the removal of Lumefantrine from contaminated waters, highlighting the novelty of the present study.

MATERIALS AND METHOD

Preparation of Lumefantrine Solution

Stock solutions were prepared by the dissolution of 1 g of Lumefantrine in 1 liter of acetone. An experimental working solution was prepared through serial dilutions. The use of acetone in the study was informed as a result of the complete solubility of the adsorbate in the organic solvent which was not obtained from most solvents. Some physiochemical properties of LUMF drug are listed in Table 1.

Sample Collection and Acid Activation of Adsorbent

Raw banana stalk samples (RBS) were collected from a farm disposal unit in Osun state, Oyan (a south-west town in Nigeria). The stalks were washed thoroughly with water and further rinsed using distilled water to remove adhering impurities. Samples were dried to constant weight. The dried stalks were pulverized, and uniform particle size was achieved using a mesh sieve. Then, carefully weighed 50 g of the pulverized samples was chemically activated with 1000 cm^3 of ortho-phosphoric acid (0.3 mol dm^{-3}). The mixture was heated and stirred continuously until a slurry was formed. The slurry formed was carbonized in an oven for 3 h at 250 °C till a char was formed. The produced char was washed with distilled water until a neutral pH was attained, after which it was oven-dried to a constant weight at 105 °C [66]. The resulting carbonized material (BSAC) was kept in an airtight container for further use.

Adsorption Assay

The batch technique was used to study the removal of Lumefantrine (LUMF) at different temperatures (303-323 K). The influence of initial operating parameters, including solution temperature, BSAC dosage, agitation time and LUMF initial concentration were critically observed. The uptake process was studied between 20-100 mg l^{-1} initial concentration of LUMF and a fixed dose of 0.1 g BSAC was used all through the adsorption experiment. 100 ml of different LUMF concentrations was put into a 200 ml flask after the adsorbent had been carefully weighed into the flask. The mixture was then agitated in a water bath shaker at 120 rpm for180 min. The samples were withdrawn at pre-set times and the residual concentrations were measured using a UV-Vis spectrophotometer at a λ_{max} of 237 nm. The amount and percentage of LUMF removed by the BSAC at equilibrium were calculated using Eqs. (1) and (2):

Table 1. Properties of Lumefantrine

Parameters	Properties
Appearance	Yellow powder
Brand name	Benflumetol
Odor	Odorless
IUPAC name	2-(Dibutylamino)-1-[(9Z)-2,7-dichloro-9[(4-chlorophunyl)methylidene]fluoren-4-yl]ethanol
Melting point	129-131 °C
Molar mass	528.942 g mol^{-1}
Molecular formula	$C_{30}H_{32}C_{l3}NO$
Solubility	Soluble in dichloromethane, acetone insoluble in water

$$q_e = \frac{C_0 - C_e}{W} \tag{1}$$

$$\%\,\mathrm{Re}moval = \frac{C_0 - C_e}{C_0} \times 100 \tag{2}$$

where q_e (in milligram/gram) is the amount of LUMF removed by BSAC, C_e (in milligram/liter) is the concentration of LUMF at equilibrium, C_o (in milligram/liter) is the initial LUMF concentration, V is the initial solution volume of LUMF (in dm^3), and W is the mass of BSAC (in grams).

Five isotherm models were used to test the experimental data, including Freundlich, Langmuir, Temkin, Dubinin-Radishkevich and Sips isotherm models. These models were employed in studying the adsorption process at equilibrium. Furthermore, the removal rate with respect to LUMF concentration in solution and details related to the adsorption mechanism were further studied using four kinetic models. Adsorption data of LUMF uptake onto the surface of BSAC was fitted into the Elovich, intraparticle diffusion (IPD), pseudo-second-order (PSO), and pseudo-first order (PFO) models, respectively. Mathematical expressions for both kinetic and isotherm models of LUMF adsorption onto BSAC are shown in Table 2.

Test of Kinetic Models

The fitness of kinetic models to adsorption data is usually described by the nearness of R^2 value to 1. Conversely, the sum of error squares (SSE) also provides a means to verify the adaptability of the kinetic models to experimental data. The applicability of the kinetic models used for this study was determined by both the R^2 values and SSE. The SSE equation is expressed in Eq. (16).

$$SSE(\%) = \sqrt{\sum \frac{\left(q_{e,\exp} - q_{e,calc}\right)^2}{N}} \tag{16}$$

Adsorption Thermodynamic Studies

The nature of interactions, spontaneity, and randomness of an adsorption process can be evaluated by available parameters from the thermodynamic studies. Parameters for the adsorption of LUMF onto BSAC are: entropy (ΔS°), enthalpy (ΔH°), and the Gibbs free energy (ΔG°). The parameters are expressed in Eqs. (17)-(19).

$$\ln K_L = \frac{\Delta S^\circ}{R} - \frac{\Delta H^\circ}{RT} \tag{17}$$

$$\Delta G^\circ = -RT \ln K_L \tag{18}$$

Table 2. Adsorption Isotherms and Kinetic Equations

Models		Mathematical expression		Ref.
Isotherm	Langmuir	$\frac{C_e}{q_e}=\frac{1}{Q_o K_L}+\frac{1}{Q_o}C_e$	(3)	[67]
		$R_L=\frac{1}{(1+K_L C_0}$	(4)	
	Freundlich	$\log q_e=\log K_f+\left(\frac{1}{n}\right)\log C_e$	(5)	[68]
	Temkin	$q_e=B\ln A_t+B\ln C_e$	(6)	[69]
		$B=\frac{RT}{b}$	(7)	
	D-R	$\ln q_e=\ln q_0-B\varepsilon^2$	(8)	[70,71,72]
		$\varepsilon=RT\ln(1+\frac{1}{C_e})$	(9)	
		$\varepsilon=\frac{1}{\sqrt{2\beta}}$	(10)	
	Sips	$\frac{1}{q_e}=\frac{1}{Q_{\max}K_s}\left(\frac{1}{C_e}\right)^{\left(\frac{1}{n}\right)}+\frac{1}{Q_{\max}}$	(11)	[73]
Kinetics	PFO	$\ln(q_e-q_t)=\ln q_e-K_1$	(12)	[74]
	PSO	$\frac{t}{q_t}=\frac{1}{k_2 q_e^2}+\frac{1}{q_e}t$	(13)	[75]
	Elovich	$q_t=\frac{1}{\beta}\ln(\alpha\beta)+\frac{1}{\beta}\ln t$	(14)	[76]
	IPD	$q_t=K_{diff}\,t^{1/2}+C$	(15)	[77]

$$\ln K_L=\ln A-\frac{E_a}{RT} \quad (19)$$

where T (K) is the absolute temperature, K_L (g l^{-1}) is the constant from the Langmuir isotherm, and R (J mol^{-1} K^{-1}) is the gas constant, E_a (kJ mol^{-1}) is the Arrhenius energy and A is the Arrhenius factor.

The plot of $\ln K_o$ *vs*. 1/T in the vant' Hoff equation gives the values of ΔH° (kJ mol^{-1}) and ΔS° (kJ mol^{-1} K^{-1}). The negative values of ΔH° and ΔS° imply that the process is exothermic and orderly at the solid-solution interface, respectively, while the positive values of both parameters imply that the process is endothermic and random at the solid-liquid interface respectively. The ΔG° values describe the spontaneity of the process at a specific temperature.

The nature of adsorption is depicted by Arrhenius expression. A sorption process is considered to be physical in nature if its E_a ranges between 5-40 kJ mol^{-1} and chemical in nature if E_a is in the range of 40-800 kJ mol^{-1}.

Effect of Solution pH

The effect of solution pH was studied by varying the initial pH from 3 to 11.01 M of HCl or NaOH solution was used in adjusting the pH of LUMF solution which was measured using a pH meter. Other operational parameters such as agitation speed, temperature, LUMF initial concentration, and BSAC dosage were kept constant.

Adsorbent Characterization

Scanning electron microscopy (SEM). SEM provides morphological information on the surface of the samples by providing images that are produced as a result of material-electron interactions. The re-emitted particles from adsorbent surfaces after bombarding by a beam of electron give rise to the working principle of the imaging technique. These dimensional images arise from the surface being analyzed as a result of the analysis of the re-emitted particles by various detectors. The textural and morphological characteristics of the adsorbent prepared in this study were investigated *via* this technique.

Fourier Transform Infrared (FTIR)

FTIR-2000 (Perkin Elmer) using a KBr disk was used to analyze the BSAC surface. The spectral characteristics related to the functional groups present on the adsorbent surface can be inferred by the spectral results obtained from the FTIR spectrophotometer.

pH and pH Point of Zero Charge (pH_{pzc})

The pH of BSAC was determined by introducing 0.1 g of adsorbent sample into a 200 ml of 0.1 M NaCl solution (of known pH). The mixture in a closed container was then agitated in a shaker at 250 rpm for 4 h. The pH was measured after agitation and the difference in pH was plotted against the initial pH. The pH_{pzc} is achieved when no charge occurs after contacting the adsorbent [78].

Boehm Titration

The Boehm titration technique was used to determine the oxygen-containing groups on the adsorbent surface [79]. 4.0 g of the adsorbent was evenly distributed into four, and each was contacted with a 15 ml solution of 0.1 M NaOH, 0.05 M Na_2CO_3, and 0.1 M $NaHCO_3$ for acidic groups and 0.1 M HCl for the basic groups. The mixture was left for 48 h at room temperature. The resulting solution was back-titrated with 0.1 M NaOH and HCl for basic and acidic groups, respectively. The nature and the type of acidic sites were calculated using previously used procedures [80].

RESULTS AND DISCUSSION

Bsac Characterization

Scanning electron micrograph (SEM). The textural characteristics of the BSAC were studied using the scanning electron microscope. Micrographs of RBS and BSAC are shown in Figs. 1a and 1b. Figure 1a shows vividly that the pores are underdeveloped, whereas Fig. 1b shows a large porosity. The observed pores in the BSAC are primarily attributed to the effect of high temperature and acid activation of BSAC which resulted in breaking down the lignocellulosic content. This is also assumed to be followed by the liberation of volatile materials in the adsorbent [78, 81, 82]. The increase in surface area and developed pores is typical of adsorbents that will effectively trap pollutant molecules [83].

Fourier Transform Infra Red Spectroscopy

The surface characteristics of the modified banana stalk sample were studied using FTIR. Spectroscopic properties of BSAC including the assignment of prominent bands to functional groups that are responsible for the adsorption process were elucidated. A possible mechanism for adsorption of LUMF on the BSAC surface was also inferred from the spectral analysis. Obvious spectra connected with certain functional groups that may support the efficient adsorption of LUMF were observed at 3012.91-3257.88 cm^{-1} (the secondary amine group), 1616.40 cm^{-1} (carbonyl group), and 3429.55 cm^{-1} (bonded O-H group) from the FTIR spectra of BSAC, as shown in Fig. 2. The influence of these prominent functional groups on the BSAC surface in removing pollutants has been reported in previous studies [84-86]. Other bands observed on the spectra which may contribute in the adsorbate uptake include 648.10 cm^{-1} (-CN stretching), 1242.20 cm^{-1} ($-SO_3$ stretching), 1114.89 cm^{-1} (-C=O=C stretching of ether) and 1402 cm^{-1} (symmetric bending of CH_3). A similar characterization result on BSAC was reported by Ogunleye *et al*. (2014) [87].

BOEHM TITRATION

Functional groups containing oxygen are oftentimes an important component of activated carbon as they influence the characteristic of carbon material surfaces [88]. Acidity and basicity of carbon material surfaces are examined by Boehm's titration which assumes that $NaHCO_3$, NaOH and Na_2CO_3 neutralize groups as the acidic groups, while

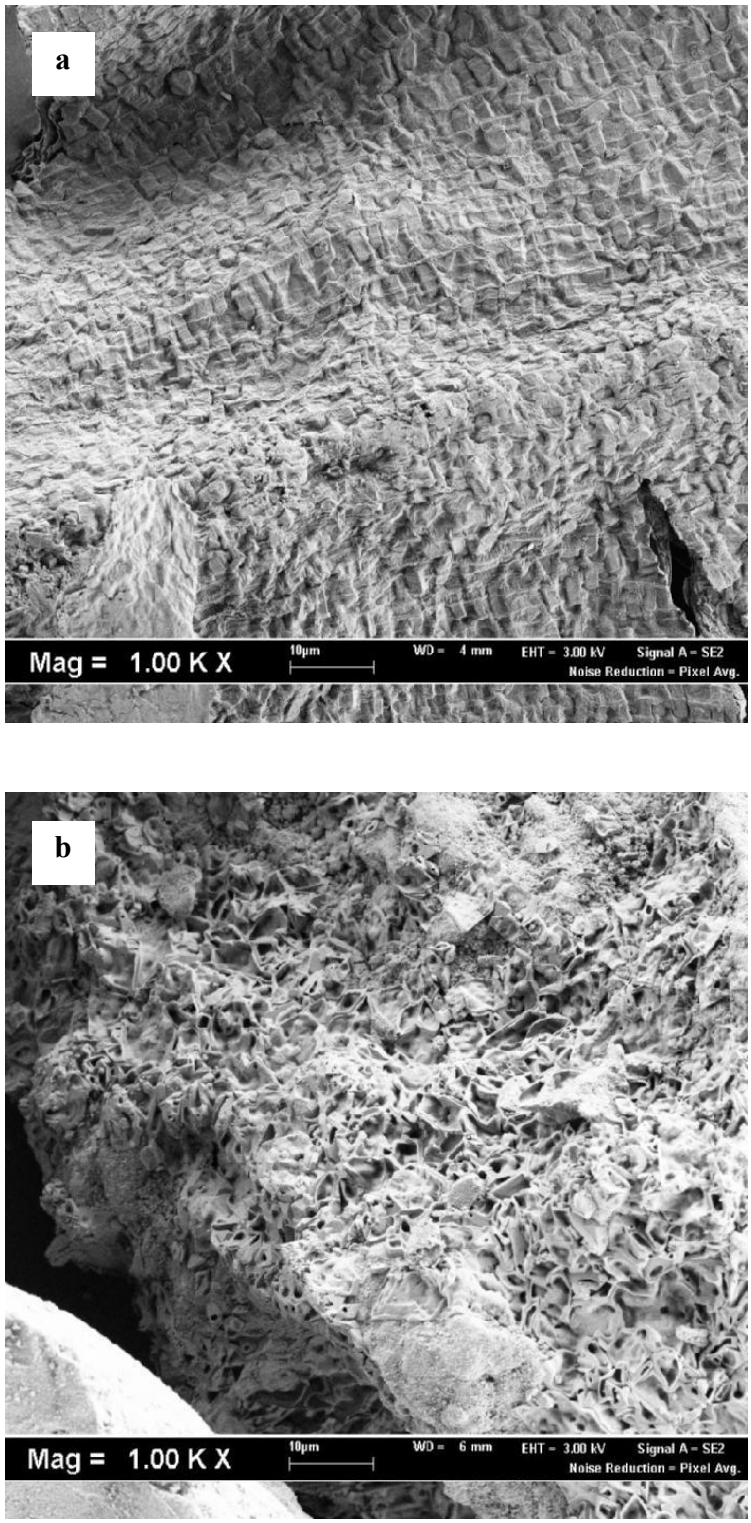

Fig. 1. SEM image of (a) RBS with 1000x magnification, (b) BSAC with 1000x magnification.

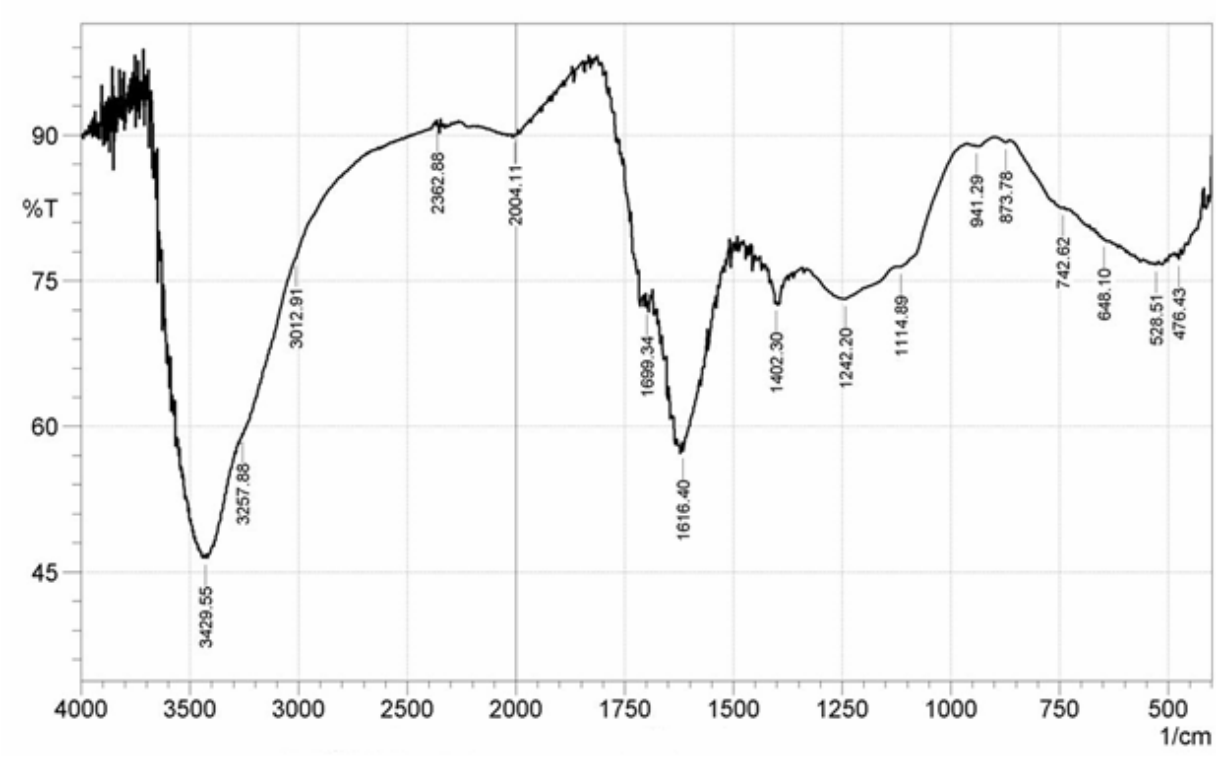

Fig. 2. FTIR spectrum of acidic modified banana stalk.

HCl neutralize groups as the basic groups. The acidic and basic groups are: carboxylic (0.1832 mmol g^{-1}), phenolic (0.2749 mmol g^{-1}), and lactonic (0.2418 mmol g^{-1}). The total basic group was 0.1582 mmol g^{-1} and that of the acidic groups was 0.699 mmol g^{-1}. It can be inferred from the results that the BSAC has more acidic groups than basic groups available on its surface. The BSAC surface is predominantly acidic as suggested by the pH_{pzc} (4.5) value obtained (Fig. 3) [89]. This indicates that the adsorption of cationic pollutants will be highly favored at this pH.

Proximate Analysis

Proximate analysis was performed using a thermogravimetric analyzer (Perkin-Elmer TGA7, USA). Results of the analysis showed that moisture, fixed carbon, volatile, and ash content for RBS were in the percentages of 14.36, 5.83, 73.91 and 5.90, respectively. Conversely, BSAC indicated low moisture and volatile contents with a high amount of fixed carbon and lower ash content with percentages of 2.91, 18.64, 73.92 and 4.53, respectively. The raw banana stalk sample showed high amount of volatile and moisture contents. During the process of activation and carbonization, organic bonds and linkages are broken leaving the volatile compounds to evaporate as liquid and gaseous products. This left the carbon material with a high carbon content [90,91]. It can be observed that the activation process led to increased fixed carbon content and a consequent decrease in the presence of volatile materials in the adsorbent.

Point of Zero Charge (pHpzc)

The results of the pH_{pzc} of BSAC are shown in Fig. 2. The point at which the curve passes through the axis of the pH_o in Fig. 2 is the pH_{pzc} which is observed at 4.5. At pHs above the pH_{pzc}, the adsorption of a cation is supported while at values below the pH_{pzc}, anionic adsorption is enhanced [78,92-94]

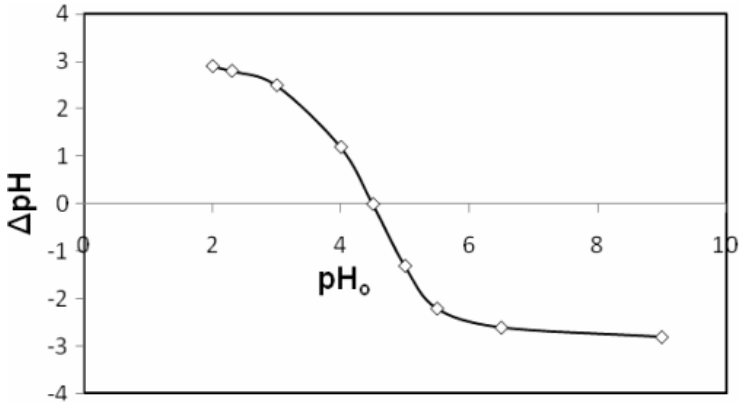

Fig. 3. Zeta potential *vs*. pH curve of BSAC.

BATCH EQUILIBRIUM STUDIES

Effects of Agitation Time, Solution Temperature, and Initial LUMF Concentration

The influence of agitation time and LUMF initial concentration is presented in Fig. 3. A rapid uptake was observed in the initial phase of 50 min contact time. Beyond this time, the adsorption rate became slower until equilibrium was attained at 120 min for all initial concentrations of LUMF, except for 20 and 40 mg l^{-1} initial concentrations in which the equilibrium was fulfilled at 70 min contact time. The difference in the equilibrium time shows the influence of the various initial LUMF concentrations on the adsorption process at large. Evidently, the adsorption rate was highly dependent on the various initial concentrations. The amount absorbed was increased with increasing the initial LUMF concentrations. Conversely, the percentage removal of LUMF decreased as initial LUMF concentration increased.

At 120 min contact time, percentage removal increased from 78% to 95% as initial LUMF concentration varied from 20 to 100 mg l^{-1}. This rapid uptake at the initial phase can be ascribed to the higher number of pores available on the BSAC surface which were occupied with adsorbate molecule, leading to a much slower adsorption rate towards equilibrium. The observed trend with the increased amount of LUMF adsorbed as initial concentrations increased, maybe due to the availability of unoccupied pores which can still accommodate more LUMF molecules. On the other hand, the decreased percentage removal observed in the same vein can be attributed to competition among adsorbate molecules to diffuse into the internal pores of the BSAC as initial concentration increases. Boudrahem *et al*. and Malakootian *et al*. reported a similar observation in the sorption of pharmaceuticals using adsorbent prepared from olive stones and pumice [95-96]. Most adsorption processes are often influenced by temperature. The uptake of LUMF increased as temperature increased from 303-323K, showing the exothermic nature of the process. The percentage and amount of LUMF removed at equilibrium were increased from 78.57% (15.714 mg g^{-1}) to 95.24% (19.048 mg g^{-1}) at 20 mg l^{-1} initial concentration even as the temperature increased from 303-323 K (Fig. 4). This notable trend is majorly attributed to the increase in surface activity [91].

Influence of pH on LUMF Adsorption

The results of pH studies on LUMF uptake by BSAC is reported in Fig. 5. The removal percentage of LUMF increased with an increase in pH from 3 to 7 and decreased generally in the basic region. At pH 3, the percentage of LUMF removal was 54.17% while at pH 7, removal was 100%. The optimum pH for this study is observed at pH 6. A 100% removal was observed at pH 5 and pH 7, but 54.167% and 86.05% were obsereved at acidic region (pH 3) and at basic region (pH 11), respectively. At pH values below the pH_{pzc} which is 4.5, the BSAC surfaces are positively charged and at higher values, it becomes charged

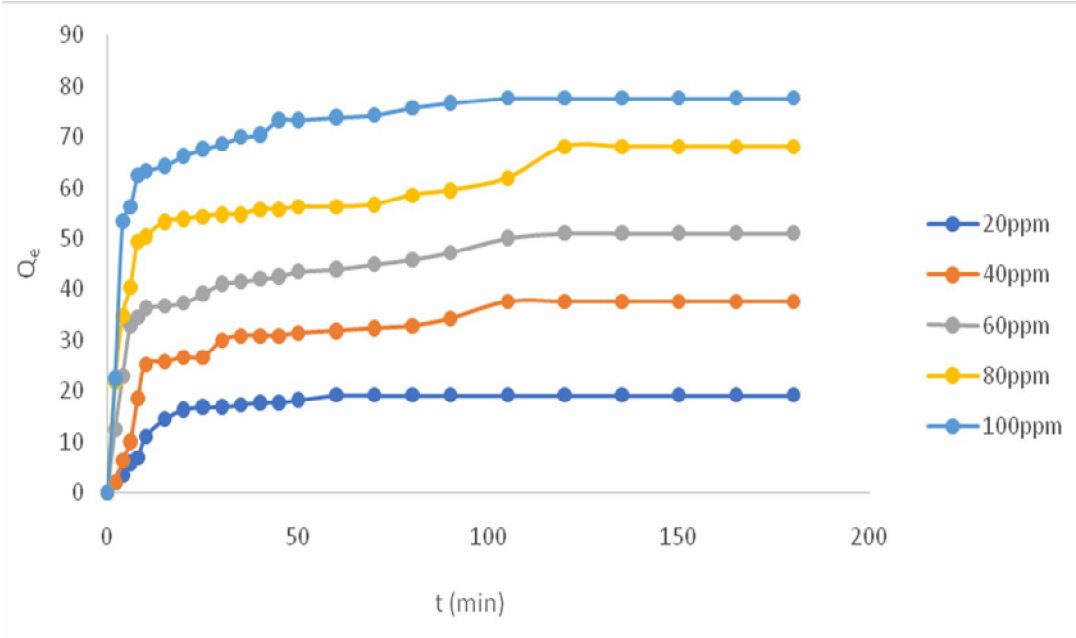

Fig. 4. The influence of agitation time and LUMF initial concentration at 323 K.

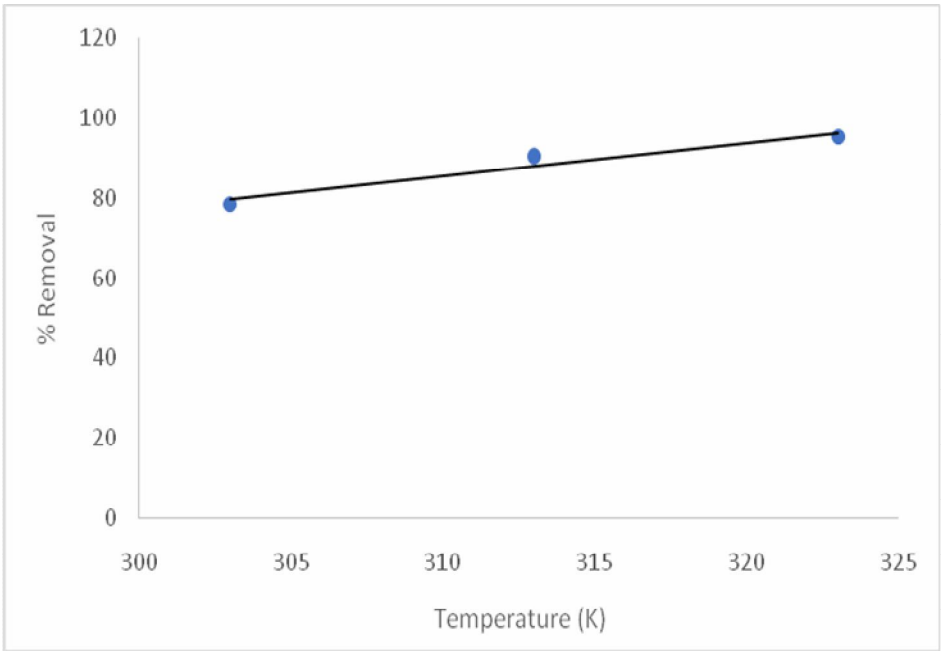

Fig. 5. Influence of temperature on the removal of LUMF by BSAC.

Table 3. The Adsorption Isotherm Constants for the Removal of LUMF Using BSAC

	Parameters	303 K	313 K	323 K
Langmuir	q_m (mg g^{-1})	98.0392	58.1395	89.2857
	K_L (l mg^{-1})	0.0948	0.25943	0.29708
	R_L	0.09542	0.03712	0.03256
	R^2	0.9998	0.9977	0.9994
Freundlich	K_f (mg g^{-1} (l mg^{-1}))$^{1/n}$	12.0726	18.2684	22.9509
	n	1.7934	2.92312	2.30097
	R^2	0.9801	0.9175	0.9316
Temkin	B_T	50.5253	98.229	62.4226
	K_t	1.03229	1.61357	1.64788
	R^2	0.9961	0.9598	0.9925
D-R	E (kJ mol^{-1})	0.70711	0.79057	1.29099
	Q_m (mg g^{-1})	57.9569	48.1297	64.6249
	R^2	0.8814	0.9199	0.9174
	B (mol^2 kJ^{-2})	1.00E-6	8.00E-07	3.00E-07
Sips	Ks	0.09506	0.2286	0.3089
	q_m (mg g^{-1})	102.1	59.6	84.14
	n	1.044	0.9986	0.9026
	R^2	1.000	0.999	0.9998

negatively [97]. Lumefantrine, a nitrogen-containing basic compound, showed an optimum adsorption between pH 5 and 7. This may be due to electrostatic interactions and hydrogen bonding between the adsorbent surface and the Lumefantrine compound. The decline in the adsorptive uptake at higher pH can be attributed to likely competition and electrostatic repulsion between the negatively charged BSAC surface and the basic Lumefantrine compound.

ADSORPTION ISOTHERM STUDIES

Five different isotherm models were used to test the adsorption data, they are: four two-parameter and one three-parameter isotherm models, respectively. The two-parameter isotherm models used are the Langmuir, D-R, Freundlich, and Temkin models while the three-parameter isotherm model used is the Sips model (Table 3). In the present study, the suitability and fitness of isotherm models to experimental data was judged according to the R^2 and q_m values obtained. The plot of the isotherm models at all temperatures studied was employed to evaluate the R^2 values and other parameters of the adsorption isotherm as shown in Table 3. The closeness of the R^2 values to unity was used to identify the most suitable isotherm model.

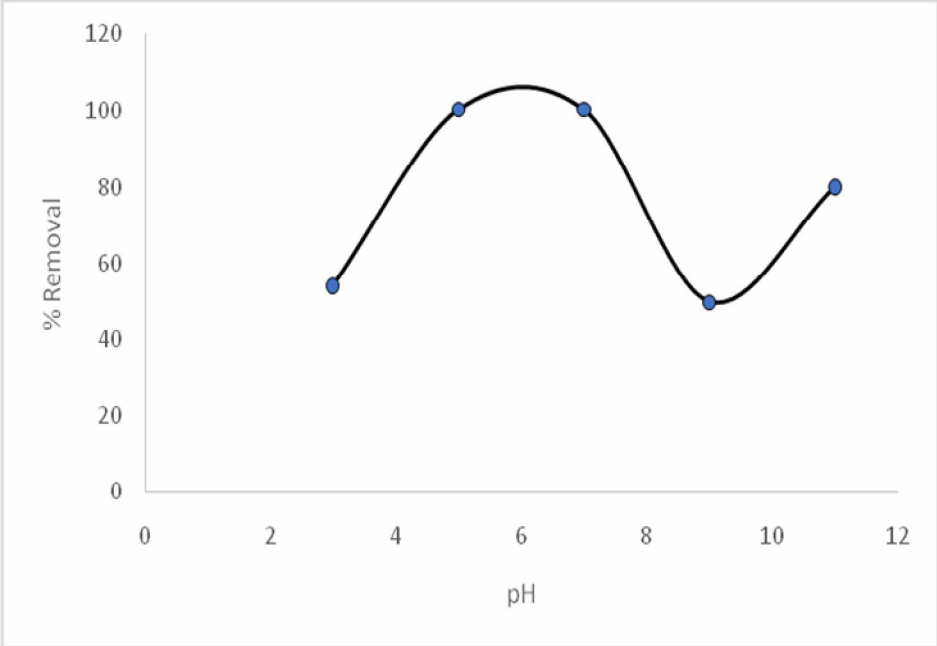

Fig. 6. Influence of pH on the adsorption of CIP by BSAC at 303 K.

Figures 6a-d shows the linearized isotherm plots for LUMF uptake at 303 K.

Maximum monolayer adsorption is commonly assumed to occur when there is monolayer coverage of the adsorbent surface by the adsorbate. The optimum monolayer adsorption capacity of BSAC can be deduced from the Langmuir isotherm. The q_m from the Langmuir model at 303 K was 98.039 mg g^{-1} with a corresponding R^2 value of 0.9998 which shows the suitability of the model in explaining the adsorption process. The separation factor (R_L) values ranging from 0.09542-0.03256 were obtained at temperatures from 303323 K. The separation factor shows the favorability of the adsorption of LUMF by BSAC as the R_L values were between 0 and 1. The n values of the Freundlich model were above 1, indicating that the process of adsorption was favorable. The adsorption energy value from the D-R isotherm was between 0.707 and 1.291 kJ mol^{-1} at all temperatures studied, suggesting physical adsorption in the removal of LUMF by BSAC. The Temkin model which assumes that the binding energies are uniformly distributed on the adsorbent surface also closely fits the experimental data judging from the closeness of its R^2 value to unity (Fig. 7).

The Sips isotherm being a combination of the Freundlich and Langmuir models gave the best fit to experimental data. Similarly, it well explains the adsorption isotherm [91]. The closer the n values of the Sips isotherm to unity, the more it tends towards the Langmuir isotherm model, suggesting monolayer adsorbate coverage on the adsorbent surface. The Sips model (Fig. 8) gave the highest q_m value of 102.1 mg g^{-1} and R^2 of 1. The values of n in the Sips isotherm were close to unity describing the adsorption data with the best fitting to the Langmuir isotherm. The fitness of the five isotherms used based on values obtained from the R^2 is in the order: Sips (1.000) > Langmuir (0.9998) > Temkin (0.9801) > D-R (0.8814).

ADSORPTION KINETIC STUDIES

To study the kinetics of the adsorption of LUMF, four different kinetic models were used. They are PSO, PFO, Elovich and IPD. Three parameters were used to ascertain the models that fit best in explaining the adsorption rate (Table 4). The parameters are the correlation coefficient

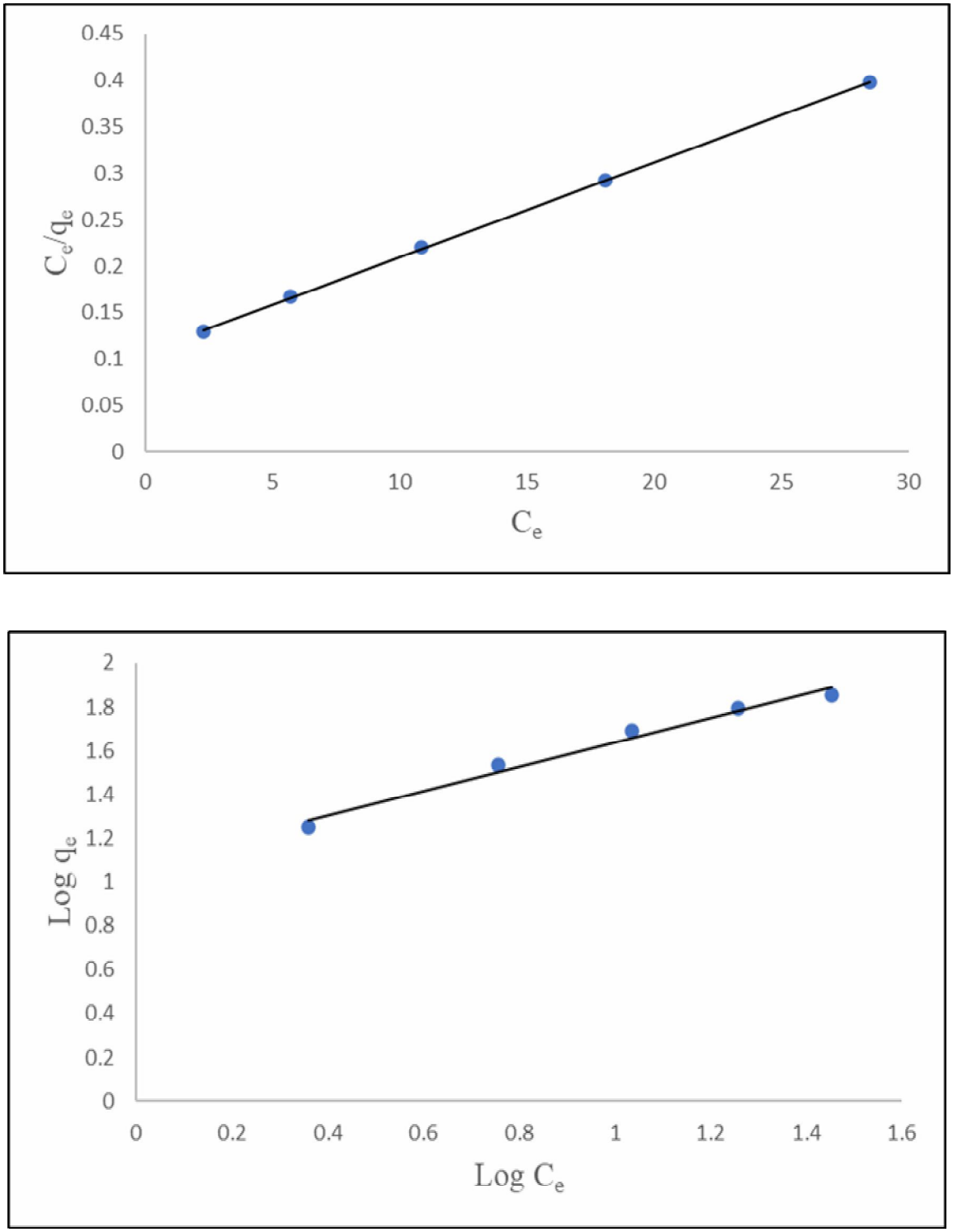

Fig. 7. Plot of Langmuir (a), Freundlich (b), Temkin (C) and D-R (d) isotherm at 303 K.

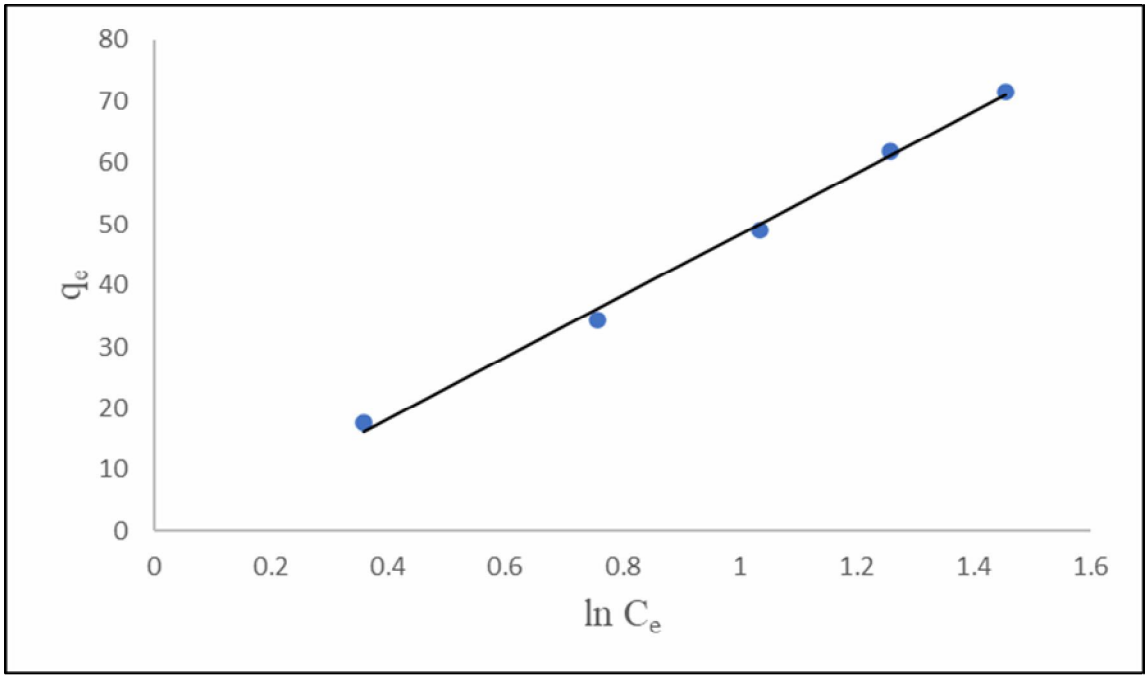

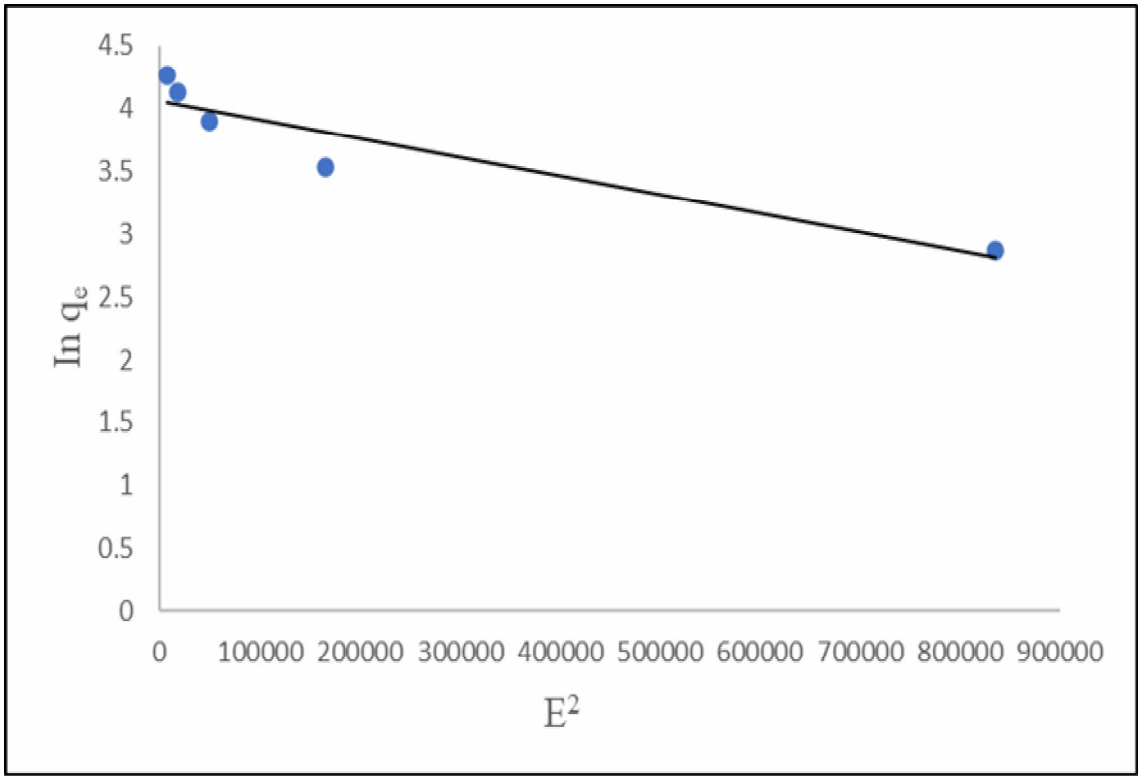

Fig. 7. Continued.

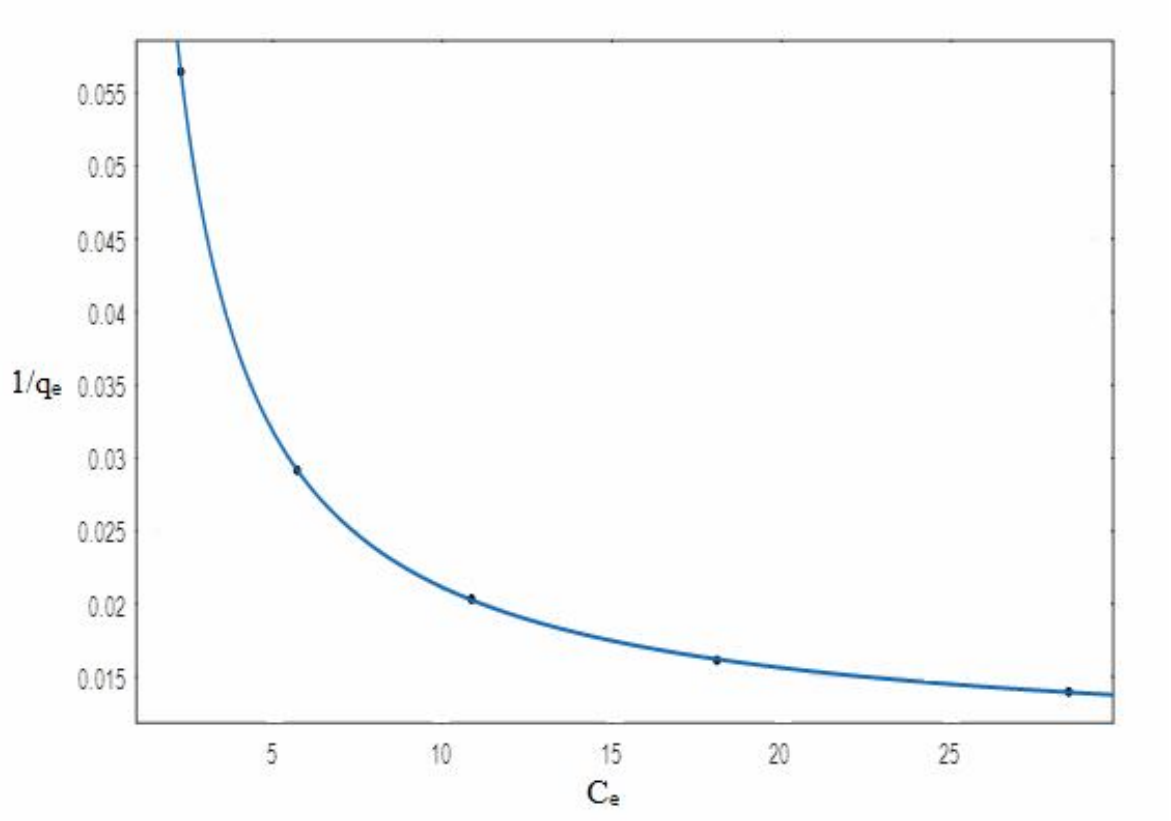

Fig. 8. Non-linear plot of the Sips isotherm at 303 K.

(R^2), the closeness of $q_{(cal)}$ to $q_{(exp)}$, and the sum of error squares (SSE). The closer the R^2 value to unity coupled with a lower SSE value describes the most suitable model for the kinetic studies. In this study, the PFO model showed R^2 value ranging from 0.5663-0.8261 and the difference in $q_{(cal)}$ and $q_{(exp)}$ ranging from 13.0311-57.8641. The SSE value ranged from 3.3646-13.275. The values obtained from the PFO model are not desirable unlike those obtained from the PSO model with R^2 values between 0.9845-0.9997 and much lower SSE values between 0.4006 and 0.9286. The PSO model shows a good fitting of the adsorption data. The low R^2 values obtained from the Elovich model make it unfit to describe the kinetics of adsorption of LUMF onto BSAC. The IPD model showed that at different initial LUMF concentrations, the plot of qt against $t^{1/2}$ did not pass through the origin as justified by the intercept obtained (Table 4). Values obtained for the intercept from the plot implies that the IPD model is likely to be the rate-limiting step but not the only mechanism responsible for the adsorption process. The Boundary layer diffusion is another possible mechanism that took place during the movement of LUMF molecules into the adsorbent. As the value of C increased (Table 4), the boundary layer effect increased as well. This provides very important details about the ability of the adsorbent to remove LUMF or be retained in solution. However, higher values of C (8.6305-41.508) imply a higher capacity for adsorption which was notably observed (Table 4) [98,99].

Adsorption Thermodynamics

The influence of temperature on LUMF uptake by BSAC is better understood by evaluating some necessary thermodynamic parameters such as the free energy, enthalpy, and entropy change. Thermodynamic parameters obtained are shown in Table 5. The endothermic nature of the adsorption of LUMF onto BSAC was noted as a positive

Table 4. Kinetic Model Parameters of LUMF Adsorption onto BSAC at 323 K

Model	Initial LUMF concentration ($mg\ l^{-1}$)				
	20	40	60	80	100
PFO					
$q_{e(exp)}$ ($mg\ g^{-1}$)	19.0476	37.619	54.9524	68.0952	77.619
$q_{e(cal)}$ ($mg\ g^{-1}$)	6.01647	20.4442	32.0886	37.9221	19.7549
k_1 (min^{-1})	0.015	0.0208	0.0215	0.0212	0.0222
R^2	0.5663	0.896	0.9173	0.8842	0.8261
SSE (%)	3.36463	3.94018	5.1125	8.08855	13.275
PSO					
$q_{e(exp)}$ ($mg\ g^{-1}$)	19.0476	37.619	54.9524	68.0952	77.619
$q_{e(cal)}$ ($mg\ g^{-1}$)	20.6186	41.6667	57.4713	69.9301	79.3651
k_2 ($g\ mg^{-1}\ min^{-1}$)	0.00484	0.00146	0.00155	0.00018	0.00341
R^2	0.9929	0.9845	0.9908	0.993	0.9997
SSE (%)	0.40561	0.92859	0.56324	0.41028	0.40057
Elovich					
B	0.24227	0.1289	0.11111	0.09866	0.0876
A	4.71237	8.31735	25.6022	60.253	116.657
R^2	0.8976	0.9381	0.9309	0.8667	0.5611
Intraparticle-diffusion					
C	5.6305	9.4769	19.271	30.005	41.508
k_{diff}	1.3422	2.6139	3.107	3.3765	3.5765
R^2	0.6866	0.7705	0.8027	0.6958	0.5611

Table 5. Adsorption Thermodynamic Parameters for LUMF Uptake onto BSAC

T (K)	K_L (M^{-1})	ΔG ($kJ\ mol^{-1}$)	ΔH ($kJ\ mol^{-1}$)	ΔS ($kJ\ mol^{-1}$)	E_a ($kJ\ mol^{-1}$)
303	31410.217	-36.2033	48.8344	0.29178	49.3536
313	85960.308	-40.0179			49.4367
323	98437.305	-41.6604			49.5198

ΔH^o value (46.83 kJ mol^{-1}). Increased disorderliness at the BSAC-LUMF interface, which suggests a favorable adsorption, was marked by a positive $\Delta S°$ value (0.242 kJ K^{-1} mol^{-1}) obtained from the thermodynamic studies. Lastly, the spontaneity of the overall process of adsorption, noted as $\Delta G°$ value (-41.66 kJ mol^{-1}), was negative. Similar reports were obtained by Tam *et al.* on the removal of diclofenac graphitic biochar [100].

Adsorption Mechanism

To understand the mode of adsorption of an adsorbate to the surface of a carbonaceous material, it is important to study its adsorption mechanism. The predictability of an adsorption mechanism can be achieved by studying the relative dependence of the process on its solution pH. The interactions between adsorbent surface and adsorbate molecules are usually influenced by the solution pH which in turn gives rise to variations in possible mechanism adoptable for various adsorption processes [101,102]. Van der Waals interactions, π-π interactions, H-bond interactions, and electrostatic interactions have been reported in previous studies to be the possible mechanisms responsible for the uptake of several pharmaceutical contaminants onto the surface of porous adsorbents [103,104].

At regions below the pH_{pzc} (4.5), the adsorbent surface is positively charged and the nitrogen group on the lumefantrine drug becomes protonated. Electrostatic repulsion at this region may have been induced, resulting in the decreased uptake observed at this pH environment. Beyond the pH_{pzc} value, the BSAC surface becomes negatively charged and just above this pH, between pH 5 and 7, the nitrogen group of lumefantrine molecules are still protonated bringing about a strong electrostatic attraction between the BSAC surface and the protonated Lumefantrine molecule (Fig. 9a). The maximum removal of the pharmaceutical at this pH range can be attributed to the strong attractive electrostatic interaction between the adsorbent and the Lumefantrine molecule. El-shafey *et al.* (2012) also reported a similar mechanism in the adsorption of CIP onto activated carbon prepared from date palm leaflets [105].

The sharp decrease in the adsorptive uptake between pH 7 and 9 is not unconnected with the deprotonation of the nitrogen group on the LUMF molecules, resulting in a strong electrostatic repulsion. The polar functional groups on the BSAC surface (carboxylic moieties) interacting by hydrogen bonding with electronegative species on LUMF molecules (O-atoms) may be responsible for the increased uptake at pH > 9 (Fig. 9b). This is also consistent with findings reported by Tam *et al.* (2019) on the removal of diclofenac from aqueous media by potassium ferrate-activated porous graphite [106]. Therefore, electrostatic interactions and hydrogen bonding are proposed as possible mechanisms for this study.

Performance Metrics Evaluation

The performance metrics of adsorbent is a parameter that can be evaluated to further ascertain the effectiveness of an adsorbents used for the uptake of pollutants without much discrepancy in the performance evaluation of such adsorbent material. The performance metrics of most adsorbents reported in previous studies have been basically evaluated based on the measurement of their adsorption capacities which are not completely dependable as certain process controlling parameters are not considered. Factors such as variation in adsorbate equilibrium concentrations usually influence the adsorption capacity of the carbon material used. At higher adsorbate concentration, a higher uptake may be recorded by the adsorbent which reduces the reliability of adsorption capacity to effectively measure an adsorbent true performance [107]. The possibility of recording a lower adsorption capacity at ambient conditions for previously reported works which have evaluated and reported efficiency based on their q_{max} is likely to occur. Therefore, to assess the performance metrics of an adsorbent, the partition coefficient (PC) method may provide a better evaluation than the adsorption capacity measurement [108,109]. The partition coefficient is the ratio of the equilibrium adsorption capacity (q_e) to the concentration at equilibrium in a solid-liquid adsorption process as shown in Eq. (20) [110],

$$Partition\ coefficient = \frac{q_e}{C_e} \tag{20}$$

where q_e is the equilibrium adsorption capacity and c_e is the concentration at equilibrium. The performance metric of the

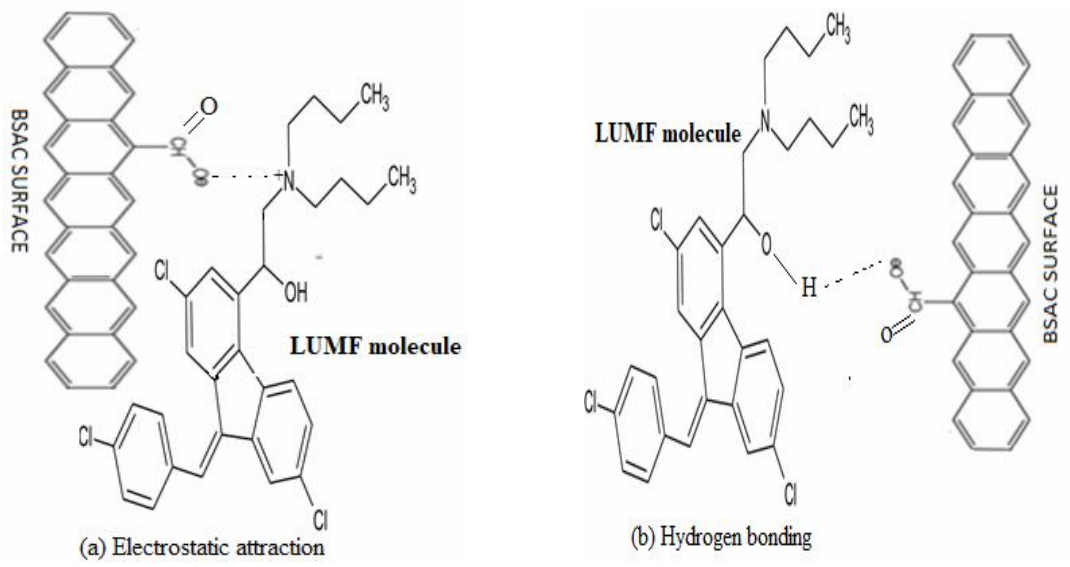

Fig. 9. Adsorption mechanism for the adsorption of LUMF unto BSAC.

Table 6. Partition Coefficient of Different Adsorbent Material for the Removal of Pharmaceuticals

Pharmaceutical pollutant	Adsorbent	Q_{max} (mg g^{-1})	Partition coefficient (PC)	Ref.
Activated carbon	Ciprofloxacin	231	12.2	[111]
Carbon nanotubes	Ciprofloxacin	135	5.6	[111]
NPC-700 derived from ZIF-8	Ciprofloxacin	416.7	0.87	[112]
Activated carbon	Diclofenac	76	0.76	[113]
18% SO_3H-UiO-66	Diclofenac	263	3.57	[113]
Carbon nanotubes	Diclofenac	33.88	1.32	[114]
PCDM-1000	Diclofenac	320	6.48	[115]
BSAC	Lumefantrine	102.1	20	This study

BSAC used in this study is therefore evaluated using the maximum adsorption capacity and the partition coefficient method. The highest percentage removal was recorded at 323 K (at 20 mg l^{-1}) and at this temperature the equilibrium adsorption capacity, was 19.04762 mg l^{-1} while the concentration at equilibrium was 0.95238 mg l^{-1}. The partition coefficient in this study is 20 which suggested a better performance of the BSAC in removing LUMF from solution. The result obtained showed that BSAC performed better that many other adsorbents used in the removal of pharmaceuticals as shown in Table 6.

Table 7. Cost Difference between BSAC and CAC

Cost description	Price (USD)	
	BSAC (1 Kg)	CAC (1 Kg)
Ortho-phosphoric acid	17.56	
Distilled water	11.86	
Electricity	4.00	
Transportation	10.00	5.0
Filter paper	3.22	
Cost of purchase	-	300
Total	46.64	305
Difference (CAC-BSAC)	258.36	

COST ANAYLSIS

The analysis of cost incurred in the course of preparing an adsorbent is important in evaluating the overall effectiveness and adoptability of the adsorbent. Comparing the prepared BSAC in this study to commercial activated carbon as described in Table 7, the BSAC is approximately five times more cost-effective than that of CAC. About USD 258 per Kg is estimated to be saved from the preparation of BSAC. A concise summary of cost incurred in the preparation of BSAC is shown in Table 7.

CONCLUSIONS

In this study, Lumefantrine was successfully removed from the solution by BSAC. Optimum conditions for the adsorption process were recorded at 120 min contact time, pH = 6, 0.1 g adsorbent dose and temperature 323 K, respectively. The optimum adsorption capacity was 102.1 mg g^{-1} with the process being thermodynamically favored. The adsorption data was best explained by the Sips isotherm and the PSO kinetic models with R^2 values of 1 or close to unity with low SSE values compared with other isotherm and kinetic models studied. The mechanism of adsorption was controlled by both intraparticle diffusion and boundary layer effect. The results obtained from this study shows that BSAC is an efficient adsorbent in removing Lumefantrine, an antimalaria drug, from solutions.

ACKNOWLEDGEMENTS

The corresponding author acknowledges the supports obtained from The World Academy of Science (TWAS) in form of Research grants; Research Grant number: 11-249 RG/CHE/AF/AC_1_UNESCO FR: 3240262674 (2012), 15-181 RG/CHE/AF/AC_1_: 3240287083 (2015) for the purchase of Research Equipments and LAUTECH 2016 TET Fund Institution Based Research Intervention (TETFUND/DESS/ UNI/OGBOMOSO/RP/VOL. IX) respectively.

REFERENCES

[1] Tam, N. T.; Liu, Y.; Bashir, H.; Yin, Z.; He, Y.; Zhou, X., Efficient removal of diclofenac from aqueous solution by potassium ferrate-activated porous graphitic biochar: Ambient condition influences and adsorption mechanism. *Int. J. Environ. Res. Public Health*. **2020**, *17*, 291. DOI: 10.3390/ijerph17010291.

[2] Houtman, C. J.; Kroesbergen, J.; Lekkerkerker-Teunissen, K.; van der Hoek, J. P., Human health risk assessment of the mixture of pharmaceuticals in dutch drinking water and its sources based on frequent monitoring data. *Sci. Total Environ.* **2014**, *496*, 54-62. DOI: 10.1016/j.scitotenv.2014.07.022.

[3] Aseel, M.; Aljeboree, A.; Alshirifi, N., Adsorption of pharmaceuticals as emerging contaminants from aqueous solutions on to friendly surfaces such as activated carbon, A review. *J. Pharm. Sci. Res.* **2018**, *10*, 2252-2257.

[4] Yeddla, R. D.; Bala, T. N.; Venkateswar., B. R, Low-cost adsorbents utilization for the treatment of pharmaceutical wastewater. *Int. J. Civ. Eng. Res.* **2017**, *8*, 39-48. DOI: 10.3311/PPch.12959.

[5] Aseel, M. A., Colorimetric determination of phenylephrine hydrochloride drug using 4-aminoantipyrine: Stability and higher sensitivity. *J. Pharm. Sci. Res.* **2018**, *10*, 1774-1779.

[6] Magner, J.; Filipovic, M.; Alsberg, T., Application of a novel solid-phase-extraction sampler and ultra-performance liquid chromatography quadrupole-time-of-flight mass spectrometry for determination of pharmaceutical residues in surface sea water. *Chemosphere*. **2010**, *80*, 1255-1260. DOI: 10.1016/j.chemosphere.2010.06.065.

[7] Bexfield, L. M.; Toccalino, P. L.; Belitz, K.; Foreman, W. T.; Furlong, E. T., Hormones and pharmaceuticals in groundwater used as a source of drinking water across the united states. *Environ. Sci. Technol.* **2019**, **53**, 2950-2960. DOI: https://doi.org/10.1021/acs.est.8b05592.

[8] Halling-Sørensen, B.; Nielsen, S. N.; Lanzky, P. F.; Ingerslev, F.; Holten Lu¨ tzhøft, H. C.; Jørgensen, S. E., Occurrence, fate and effects of pharmaceutical substances in the environment. A review, *Chemosphere*. **1998**, *36*, 357-393. DOI: https://doi.org/10.1016/S0045-6535(97)00354-8.

[9] Jones, O. A.; Lester, J. N.; Voulvoulis, N., Pharmaceuticals: A threat to drinking water. *Trends Biotechnol.* **2005**, *23*, 163-167. DOI: 10.1016/j.tibtech.2005.02.001.

[10] Pal, R.; Megharaj, M.; Kirkbride, K. P.; Naidu, R., Illicit drugs and the environment, A review. *Sci. Tot. Environ.* **2013**, *463-464*, 1079-1092. DOI: 10.1016/j.scitotenv.2012.05.086.

[11] Deblonde, T.; Cossu-Leguille, C.; Hartemann, P., emerging pollutants in wastewater, A review of the literature. *Int. J. Hyg. Environ. Health*. **2011**, *214*, 442-448. DOI: 10.1016/j.ijheh.2011.08.002.

[12] Fatta-Kassinos, D.; Ku¨ Mmerer, K., Pharmaceuticals in the environment, sources, fate, effects and risks. *Environ. Sci. Pollut. Res.* **2010**, *17*, 519-521.

[13] Gunnarsdo´ttir, R.; Jenssen, P. D.; Erland Jensen, P.; Villumsen, A.; Kallenborn, R., A review of wastewater handling in the Arctic with special reference to pharmaceuticals and personal care products (PPCPs) and microbial pollution. *Ecol. Eng*. **2013**, *50*, 76-85.

[14] Azizullah, A.; Khattak, M. N.K.; Richter, P.; Ha¨der, D. -P., Water pollution in Pakistan and its impact on public health, A review. *Environ. Int.* **2011**, *37*, 479-497. DOI: 10.1016/j.envint.2010.10.007.

[15] Heberer, T., Occurrence, fate and removal of pharmaceutical residues in the aquatic environment: A review of recent research data. *Toxicol. Lett.* 2002, *131*, 5-17. DOI: 10.1016/s0378-4274(02)00041-3.

[16] Tolls, J., Sorption of veterinary pharmaceuticals in soils, A review. *Environ. Sci. Technol.* ***2001***, *35*, 3397-3406. DOI: https://doi.org/10.1021/es0003021.

[17] Ort, C.; Lawrence, M. G.; Rieckermann, J.; Joss, A., Sampling for pharmaceuticals and personal care products (PPCPs) and illicit drugs in wastewater systems, Are your conclusions valid? A critical review. *Environ. Sci. Technol.* **2010**, *44*, 6024-6035. DOI: https://doi.org/10.1021/es100779n.

[18] Kaplan, S., Review: Pharmacological pollution in water. *Crit. Rev. Environ. Sci. Technol.* **2012**, *43*, 1074-1116. DOI: https://doi.org/10.1080/10934529.2011.627036.

[19] Liu, J. -L.; Wong, M. H., Pharmaceuticals and personal care products (PPCPs), A review on environmental contamination in China. *Environ. Int.* **2013**, *59*, 208-224. DOI: https://doi.org/10.1016/j.envint.2013.06.012.

[20] Gadipelly, C.; Pérez-González, A.; Yadav, G. D.;

Ortiz, I.; Ibánez, R.; Rathod, V. K.; Marathe, K. V., Pharmaceutical industry wastewater, review of the technologies for water treatment and reuse. *Ind. Eng. Chem. Res.* **2014**, *53*, 11571-11592. DOI: https://doi.org/10.1021/ie501210j.

[21] Bhagawan, D.; Poodari, S.; Pothuraj, T.; Srinivasulu, D.; Shankaraiah, G.; Yamuna, R. M.; Himabindu, V.; Vidyavathi, S., Removal of heavy metals from electroplating waste water by electro coagulation, case study. *Environ. Sci. Pollut. Research.* **2014**, *10*, 11356-3331.

[22] Andrade, J. R.; Oliveira, M. F.; da Silva, M. C.; Vieira, M. G., Adsorption of pharmaceuticals from water and wastewater using nonconventional low-cost materials, A Review. *Ind. Eng. Chem. Res.* **2018**, *57*, 3103-3127. DOI: https://doi.org/10.1021/acs.iecr.7b05137.

[23] Grassi, M.; Kaykioglu, G.; Belgiorno, V.; Lofrano, G., Removal of Emerging Contaminants from Water and Wastewater by Adsorption Process, in Emerging Compounds Removal from Wastewater. Ed.; Springer Netherlands. **2012**, pp. 15-37.

[24] Tong, D. S.; Zhou, C. H.; Lu, Y.; Yu, H.; Zhang, G. F.; Yu, W. H., Adsorption of acid red G dye on octadecyl trimethylammonium montmorillonite. *Appl. Clay Sci.* **2010**, *50*, 427-431. DOI: https://doi.org/10.1016/j.clay.2010.08.018.

[25] Priya, B.; Gupta, V. K.; Pathania, D.; Singha, A. S., Synthesis, characterization and antibacterial activity of biodegradable starch/PVA composite films reinforced with cellulosic fibre. *Carbohydrate Polymer.* **2014**, *109*, 171-179. DOI: https://doi.org/10.1016/j.carbpol.2014.03.044.

[26] Dil, E. A.; Ghaedi, M.; Ghaedi, A. M.; Asfaram, A.; Goudarzi, A.; Hajati, S.; Agarwal, M. S.; Gupta, V. K., Modeling of quaternary dyes adsorption onto ZnO-NR-AC artificial neural network: Analysis by derivative spectrophotometry. *J. Ind. Engin. Chem.* **2016**, *34*, 186-197. DOI: https://doi.org/10.1016/j.jiec.2015.11.010

[27] Gupta, V. K.; Carrott, P. J. M.; Singh, R.; Chaudhary, M.; Kushwaha, S., Cellulose: A review as natural, modified and activated carbon adsorbent. *Bio. Technol.* **2015**, *216*, 1066-1076. DOI: https://doi.org/10.1016/j.biortech.2016.05.106.

[28] Nekouei, F.; Nekouei, S.; Tyagi, I.; Gupta, V. K., Kinetic, thermodynamic and isotherm studies for acid blue 129 removal from liquids using copper oxide nanoparticle-modified activated carbon as a novel adsorbent. *J. Mol. Liquids.* **2015**, *201*, 124-133. DOI: https://doi.org/10.1016/j.molliq.2014.09.027.

[29] Gupta, V. K.; Rastogi, A.; Dwivedi, M. K.; Mohan, D., Process development for the removal of zinc and cadmium from wastewater using slag-A blast furnace waste material. *Sep. Sci. Technol.* **1997**, *32*, 2883-2912. DOI: https://doi.org/10.1080/01496399708002227.

[30] Gupta, V. K.; Saleh, T. A., Sorption of pollutants by porous carbon, carbon nanotubes and fullerene- an overview. *Environ. Sci. Pollut. Res.* **2013**, *20*, 1261-1268. DOI: 10.1007/s11356-013-1524-1.

[31] Mittal, A.; Mittal, J.; Malviya, A.; Gupta, V. K., Removal and recovery of chrysoidine Y from aqueous solutions by waste materials. *J. Coll. Inter. Sci.* **2010**, *344*, 497-507. DOI: 10.1016/ j.jcis.2010.01.007.

[32] Gupta, V. K.; Jain, R.; Nayak, A.; Agarwal, S.; Shrivastava, M., Removal of the hazardous dye-tartrazine by photodegradation on titanium dioxide surface. *Mater. Sci. Engin: C.* **2011**, *31*, 1062-1067. DOI: http://dx.doi.org/10.1016/j.msec.2011.03.006.

[33] Saleh, T. A.; Gupta, V. K., Photo-catalyzed degradation of hazardous dye methyl orange by use of a composite catalyst consisting of multi-walled carbon nanotubes and titanium dioxide, *J. Coll. Inter. Sci.* **2012**, *371*, 101-106. DOI: 10.1016/ j.jcis.2011.12.038.

[34] Gupta, V. K.; Nayak, A.; Agarwal, S., Bioadsorbents for remediation of heavy metals: Current status and their future prospects. *Environ. Engin. Res.* **2015**, *20*, 001-018. DOI: https://doi.org/10.4491/eer.2015.018.

[35] Saleh, T. A.; Gupta, V. K., Processing methods, characteristics and adsorption behavior of tire derived carbons: a review. *Adv. Coll. Inter. Sci.* **2014**, *211*, 92-100. DOI: 10.1016/j.cis.2014.06.006.

[36] Saravanan, R. Sacari, E.; Gracia, F.; Khan, M. M.;

Mosquera, E.; Gupta, V. K., Conducting PANI stimulated ZnO system for visible light photocatalytic degradation of coloured dyes. *J. Mol. Liq*. **2016**, *221*, 1029-1033. DOI: https://doi.org/10.1016/j.molliq.2016.06.074.

[37] Rajendran, S.; Khan, M. M.; Gracia, F.; Qin, J.; Gupta, V. K.; Arumainathan S., Ce(3+)-ion-induced visible-light photocatalytic degradation and electrochemical activity of ZnO/CeO_2 nanocomposite. *Scientific Reports* **2016**, *6*, 31641. DOI: 10.1038/srep31641.

[38] Saravanan, R.; Karthikeyan, S.; Gupta, V. K.; Sekaran, G.; Narayanan V., Enhanced photocatalytic activity of ZnO/CuO nanocomposite for the degradation of textile dye on visible light illumination. *Mat. Sci. Engin. C*. **2013**, *33*, 91-98. DOI: 10.1016/j.msec.2012.08.011.

[39] Saravanan, R.; Thirumal, E.; Gupta, V. K.; Narayanan, V.; Stephen, A., The photocatalytic activity of ZnO prepared by simple thermal decomposition method at various temperatures. *J. Mol. Liq*. **2013**, *177*, 394-401. DOI: https://doi.org/10.1016/j.molliq.2012.10.018.

[40] Saravanan, R.; Gupta, V. K.; Prakash, T.; Narayanan, V.; Stephen, A., Synthesis, characterization and photocatalytic activity of novel Hg doped ZnO nanorods prepared by thermal decomposition method, *J. Mol. Liq*. **2013**, *178*, 88-93. DOI: https://doi.org/10.1016/j.molliq.2012.11.012.

[41] Saleh, T. A.; Gupta, V. K., Functionalization of tungsten oxide into MWCNT and its application for sunlight-induced degradation of rhodamine B. *J. Coll. Inter. Sci.,* **2011**, *362*, 337-344. DOI: https://doi.org/10.1016/j.jcis.2011.06.081.

[42] Saleh, T. A.; Gupta, V. K., Photo-catalyzed degradation of hazardous dye methyl orange by use of a composite catalyst consisting of multi-walled carbon nanotubes and titanium dioxide. *J. Coll. Inter. Sci.* **2011**, *371*, 101-106. DOI: 10.1016/ j.jcis.2011.12.038.

[43] Gupta, V. K.; Sharma, S., Removal of zinc from aqueous solutions using bagasse fly fsh-a low cost adsorbent, *Ind. Engin. Chem. Res.* **2003**, *42*, 6619-6624. DOI: https://doi.org/10.1021/ie0303146.

[44] Ahmaruzzaman, M.; Gupta, V. K., Rice husk and its ash as low-cost adsorbents in water and Wastewater Treatment. *Ind. Engin. Chem. Res.* **2011**, *50*, 13589-13613. DOI: https://doi.org/10.1021/ie201477c.

[45] Mohammadi, N.; Khani, H.; Gupta, V. K.; Amereh, E.; Agarwal, S., Adsorption process of methyl orange dye onto mesoporous carbon material-kinetic and thermodynamic studies. *J. coll. Inter. Sci.* **2011**, *362*, 457-462. DOI: 10.1016/j.jcis.2011.06.067.

[46] Saleh, T. A.; Gupta, V. K., Synthesis and characterization of alumina nano-particles polyamide membrane with enhanced flux rejection performance. *Sep. Purify. Techol.* **2012**, *89*, 245-251 DOI: https://doi.org/10.1016/j.seppur.2012.01.039.

[47] Saravanan, R.; Khan, M. M.; Gupta, V. K.; Mosquera, E.; Gracia, F.; Narayanan, V.; Stephen, A., ZnO/Ag/CdO nanocomposite for visible light-induced photocatalytic degradation of industrial textile effluents. *J. Coll. Inter. Sci.* **2015**, *452*, 126-133. DOI: 10.1016/j.jcis.2015.04.035.

[48] Saravanan, M.; Khan, M.; Gupta, V. K.; Mosquera, E.; Gracia, F.; Narayanan, V.; Stephen, A., ZnO/Ag/Mn_2O_3 nanocomposite for visible light-induced industrial textile effluent degradation, uric acid and ascorbic acid sensing and antimicrobial activity. *RSC Advances.* **2015**, *5*, 34645-34651. https://doi.org/10.1039/C5RA02557E.

[49] Ghaedi, M.; Hajjati, S.; Mahmudi, Z.; Tyagi, I.; Agarwal, S.; Maity, A.; Gupta, V. K., Modeling of competitive ultrasonic assisted removal of the dyes-methylene blue and Safranin-O using Fe_3O_4 nanoparticles. *Chem. Engin. Jour.* **2015**, *268*, 28-37. DOI: https://doi.org/10.1016/j.cej.2014.12.090.

[50] Gupta, V. K.; Nayak, A.; Agarwal, S.; Tyagi I., Potential of activated carbon from waste rubber tire for the adsorption of phenolics, Effect of pre-treatment conditions. *J. Coll. Inter. Sci.* **2014**, *417*, 420-430. DOI: 10.1016/j.jcis.2013.11.067.

[51] Saravanan, R.; Joicy, S.; Gupta, V. K.; Narayanan, V., Visible light induced degradation of methylene blue using CeO_2/V_2O_5 and CeO_2/CuO catalysts.

Mater. Sci. Engin. C **2013**, *33*, 4725-4731. DOI: 10.1016/j.msec.2013.07.034.

[52] Saravanan, R.; Karthikeyan, N.; Gupta, V. K.; Thirumal, E.; Thangadurai, P.; Narayanan, V.; Stephen, A., ZnO/Ag nanocomposite: An efficient catalyst for degradation studies of textile effluents under visible light. *Mater. Sci. Engin. C.* **2013**, *33*, 2235-2244. DOI: 10.1016/j.msec.2013.01.046.

[53] Saravanan, R. M.; Khan, M.; Gupta, V. K.; Mosquera, E.; Gracia, F.; Narayanan, V.; Stephen, A., nO/Ag/CdO nanocomposite for visible light-induced photocatalytic degradation of industrial textile effluents. *J. Coll. Inter. Sci.* **2015**, *452*, 126-133. DOI: 10.1016/j.jcis.2015.04.035.

[54] Asfaram, A.; Ghaedi, M.; Agarwal, S.; Tyagi, I.; Gupta, V. K., Removal of basic dye auramine-O by ZnS:Cu nanoparticles loaded on activated carbon: optimization of parameters using response surface methodology with central composite design. *RSC Advances.* **2015**, *5*, 18438-18450. DOI: https://doi.org/10.1039/C4RA15637D.

[55] Gupta, V. K.; Atar, N.; Yola, M. L.; Üstündağ, Z.; Uzun, L., A novel magnetic Fe@Au core-shell nanoparticles anchored graphene oxide recyclable nanocatalyst for the reduction of nitrophenol compounds. *Wat. Res.* **2014**, *48*, 210-217. DOI: https://doi.org/10.1016/j.watres.2013.09.027.

[56] Gupta, V. K.; Jain, C.K.; Ali, I.; Chandra, S.; Agarwal, S., Removal of lindane and malathion from wastewater using bagasse fly ash-a sugar industry waste. *Wat. Res.* **2002**, *36*, 2483-2490. DOI: https://doi.org/10.1016/S0043-1354(01)00474-2.

[57] Saravanan, R.; Gupta, V. K.; Narayanan, V.; Stephen, A., Comparative study on photocatalytic activity of ZnO prepared by different methods. *J. Mol. Liq.* **2013**, *181*, 133-141. DOI: https://doi.org/10.1016/j.molliq.2013.02.023.

[58] Nodeh , H. R.; Ibrahim, W. A. W.; Ali, I.; Sanagi, M. M., Development of magnetic graphene oxide adsorbent for the removal and preconcentration of As(III) and As(V) species from environmental water samples. *Environ. Sci. Poll. Res.* **2016**, *23*, 9759-9773. DOI: 10.1007/s11356-016-6137-z.

[59] Ali, I.; Gupta, V. K.; Khan, T. A.; Asim, M., Removal of arsenate from aqueous solution by electro coagulation method using Al-Fe electrodes. Inter. J. Electro. Sci. **2012**, 7, 1898-1907.

[60] Devaraj, M.; Saravanan, R.; Deivasigamani, R. K.; Gupta, V.K.; Gracia, F.; Jayadevan, S., Fabrication of novel shape Cu and Cu/Cu_2O nanoparticles modified electrode for the determination of dopamine and paracetamol. *J. Mol. Liq.* **2016**, *221*, 930-941. DOI: https://doi.org/10.1016/j.molliq.2016.06.028.

[61] Burakov, A. E.; Galunin, E. V.; Burakova, I. V.; Kucherova, A. E.; Agarwal, S.; Tkachev, A. G.; Gupta, V. K., Adsorption of heavy metals on conventional and nanostructured materials for wastewater treatment purposes: A review. *Eco. Environ. Safety.* **2018**, *148*, 702-712. DOI: https://doi.org/10.1016/j.ecoenv.2017.11.034.

[62] Gupta, V. K.; Saleh, T. A., Sorption of pollutants by porous carbon, carbon nanotubes and fullerene- an overview. *Environ. Sci. Poll. Res.* **2013**, *20*, 2828-2843. DOI: 10.1007/s11356-013-1524-1.

[63] Ali, I.; Burakova, I.; Galunin, E.; Burakov, A.; Mkrtchyan, E.; Melezhik, A.; Kurnosov, D.; Tkachev, A.; Grachev, V., High-speed and high-capacity removal of methyl orange and malachite green in water using newly developed mesoporous carbon: Kinetic and isotherm studies. *ACS Omega.* **2019**, *4*, 19293-19306. DOI: 10.1021/ acsomega.9b02669.

[64] Nekouei, F.; Nekouei, S.; Tayagi, I. J.; Gupta, V. K., Kinetic, thermodynamic and isotherm studies for acid blue 129 removal from liquids using copper oxide nanoparticle-modified activated carbon as a novel adsorbent. *J. Mol. Liquids* **2014**, *198*, 409-412.

[65] Ali, I.; Alexandr, E. B.; Alexandr, V. M.; Alexandr, V. B.; Irina, V. B.; Elena, A. N.; Evgeny, V. G.; Alexey, G. T.; Denis, V. K., Removal of copper(II) and zinc(II) ions in water on a newly synthesized polyhydroquinone/graphene nanocomposite material: Kinetics, thermodynamics and mechanism. *Chem. Select* **2019**, *4*, 12708-12718. DOI: 10.1002/slct.201902657.

[66] Olakunle, M. O.; Inyinbor, A. A.; Dada, A. O.; Bello, O. S., Combating dye pollution using cocoa

pod husks: a sustainable approach. *Int. J. Sustain. Eng*. **2017**, *11*, 4-15. DOI: 10.1080/19397038.2017.1393023.

[67] Langmuir, I., The adsorption of gases on plane surfaces of glass, mica and platinum, *J. Am. Chem. Soc.* **1918**, *40*, 1361-1403. DOI: https://doi.org/10.1021/ja02242a004.

[68] Freundlich, H.M., Over the adsorption in solution. *J. Phys. Chem.* **1906**, *57*, 385-470.

[69] Temkin, M.; Pyzhev, V., Kinetics of ammonia synthesis on promoted iron catalysts. Acta physiochim. *URSS* **1940**, *12*, 217-222.

[70] Dubinin, M. M., The potential theory of adsorption of gases and vapors for adsorbents with energetically non-uniform surface. *Chem. Rev.* **1960**, *60*, 235-266. DOI: https://doi.org/10.1021/cr60204a006.

[71] Ajemba, R. O., Adsorption of malachite green from aqueous solution using activated ntezi clay: optimization. Isotherm and Kinetic Studies. *Int. J. Eng*. **2014**, *27*, 839-854. DOI: 10.5829/idosi.ije.2014.27.06c.03.

[72] Ojedokun, A. T.; Bello, O. S., Kinetic modeling of liquid-phase adsorption of Congo red dye using guava leaf-based activated carbon. *Appl. Water Sci.* **2017**, *7*, 1965-1977. DOI: 10.1007/s13201-015-0375-y.

[73] Sips, R., Combined form of Langmuir and Freundlich equations. *J. Chem. Phys.* **1948**, *16*, 490-495. DOI: https://doi.org/10.1063/1.1746922.

[74] Lagergren, S.; der sogenannten, Z. T.; Stoffe, G.; Handl, V., *Adsorption*. **1898**, *24*, 1-39.

[75] Ho, Y. S.; McKay, G., Pseudo-second order model for sorption processes. *Proc. Biochem*. **1999**, *34*, 451-465. DOI: 10.1016/S0032-9592(98)00112-5.

[76] Aharoni, C.; Ungarish, M., Kinetics of activated chemisorptions, Part I: The non-Elovichian part of the isotherm. *J. Chem. Soc. Farad Trans.* **1976**, *72*, 265-268. DOI: 10.1039/F19767200400.

[77] Weber, W. J.; Morris, J. C., Kinetics of adsorption on carbon from solution. J. Sanit. Eng, Div. ASCE **1962**, 89, 31-59.

[78] Bello, O. S.; Owojuyigbe, E. S.; Babatunde, M. A.; Folaranmi, F. E., Sustainable conversion of agro-wastes into useful adsorbents. *Appl. Water Sci.* **2017**, *7*, 3561-3571. DOI: 10.1007/s13201-016-0494-0.

[79] Boehm, H. P., Surface oxides on carbon and their analysis: a critical assessment. *Carbon*. **2002**, *40*, 145-149. DOI: 10.1016/S0008-6223(01)00165-8.

[80] Bello, O. S.; Lasisi, B. M.; Adigun, O. J.; Ephraim, V., Scavenging Rhodamine B dye using Moringa oleifera seed pod. *Chem. Spec. Bio*. **2017**, *29*, 120-134. DOI: 10.1080/09542299.2017.1356694.

[81] Bello, O. S.; Siang, T. T.; Ahmad, M. A., Adsorption of remazol brilliant violet-5R reactive dye from aqueous solution by cocoa pod husk-based activated carbon: kinetic, equilibrium and thermodynamic studies. *Asia Pac J. Chem. Eng*. **2012**, *7*, 378-388. DOI: https://doi.org/10.1002/apj.557.

[82] Bello, O. S.; Adegoke, K. A.; Fagbenro, S. O.; Lameed, O. S., Functionalized coconut husks for Rhodamine-B dye sequestration. *Appl. Water Sci.* **2019**, *189*, 1-15. DOI: 10.1007/s13201-019-1051-4.

[83] Ahmad, M. A.; Afandi, N. S.; Adegoke, K. A.; Bello, O. S., Optimization and batch studies on adsorption of malachite green dye using rambutan seed activated carbon. *Desalin. Water Treat.* **2016**, *57*, 21487-21511. DOI: 10.1080/19443994.2015.1119744.

[84] Hossain, M. A.; Ngo, H. H.; Guo, W. S.; Nguyen, T. V., Biosorption of Cu(II) from water by banana peel based biosorbent: experiments and models of adsorption and desorption. *J. Water Sustain*. **2012**, *2*, 87-104.

[85] Wu, H. X.; Wang, T. J.; Chen, L.; Jin, Y., The roles of the surface charge and hydroxyl group on a Fe-Al-Ce adsorbent in fluoride adsorption. Ind. *Eng. Chem. Res.* **2009**, *48*, 4530-4534. DOI: 10.1021/ie800890q.

[86] MohdYasim, N. S.; Ismail, Z. S.; MohdZaki, S.; Abd Azis, M., Adsorption of Cu, As, Pb and Zn by banana trunk. *Malaysian J. Anal. Sci.* **2016**, *20*, 187-196. DOI: 10.17576/mjas-2016-2001-20.

[87] Ogunleye, O. O.; Adio, O.; Salawudeen, T. O., Removal of lead(II) from aqueous solution using banana (musa paradisiaca) stalk-based activated carbon. *Chem. Pro. Eng. Res.* **2014**, *28*, 45-59.

[88] Budinova, T.; Ekinci, E.; Yardim, F.; Grimm, A.;

Björnbom, E.; Minkova, V.; Goranova, M., Characterization and application of activated carbon produced by H_3PO_4 and water vapor activation. *Fuel Process. Technol.* **2006**, *87*, 899-905. DOI: 10.1016/j.fuproc.2006.06.005.

[89] Bello, O. S.; MohdAzmier, A.; Ahmad, N., Adsorptive features of banana (Musa paradisiaca) stalk-based activated carbon for malachite green dye removal. *Chem. Eco*. **2012**, *28*, 153-167. DOI: 10.1080/02757540.2011.628318.

[90] Ahmad, M. A.; Alrozi, R., Optimization of preparation conditions for mangosteen peel-based activated carbons for the removal of remazol brilliant blue R using response surface methodology. *Chem. Eng. J.* **2010**, *165*, 883-890. DOI: 10.1016/j.cej.2010.10.049.

[91] Ahmad, M.; Ahmad, N.; Bello, O. S., Modified durian seed as adsorbent for the removal of methyl red dye from aqueous solutions. *Appl Water Sci.* **2015**, *5*, 407-423. DOI: 10.1007/s13201-014-0208-4.

[92] Almeida, C. A. P.; Debacher, N. A.; Downs, A. J., Removal of methylene blue from coloured effluents by adsorption on montmorillonite clay. *J. Colloid. Interface Sci.* **2009**, *332*, 46-53. DOI: 10.1016/j.jcis.2008.12.012.

[93] Farahani, M.; Abdullah, S.; Hosseini, S., Adsorption-based cationic dyes using the carbon active sugarcane bagasse. *Proc Environ Sci.* **2011**, *10*, 203-208. DOI: 10.1016/j.proenv.2011.09.035.

[94] Hamadaou, O., Removal of Rhodamine B from aqueous solutions by tea waste. *J. Hazard. Mater.* **2006**, *135*, 264-273.

[95] Boudrahem, F.; Yahiaoui, I.; Saidi, S.; Yahiaoui, K.; Kaabache, L.; Zennache, M.; Aissani-Benissad, F., Adsorption of pharmaceutical residues on adsorbents prepared from olive stones using mixture design of experiments model. *Water Sci. Technol.* **2019**, *80*, 998-1009. DOI: 10.2166/wst.2019.346.

[96] Malakootian, M.; Bahraini, S.; Malakootian, M.; Zarrabi, M., Removal of tetracycline antibiotic from aqueous solutions using natural and modified pumice with magnesium chloride. *Adv. Environ. Biol.* **2016**, *10*, 46-56.

[97] Farahani, M.; Abdullah, S. R. S.; Hosseini, S., Adsorption-based cationic dyes using the carbon active sugarcane bagasse. *Procedia Environ. Sci. (Part A)* **2011**, *10*, 203-208. DOI: 10.1016/j.proenv.2011.09.035.

[98] Ozcan, A. S.; Erdem, B.; Ozcan, A., Adsorption of acid blue 193 from aqueous solutions onto BTMA-bentonite. *Colloid. Surf. A Phys. Eng. Asp.* **2005**, *266*, 73-81. DOI: 10.1016/j.jcis.2004.07.035.

[99] Namasivayam, C.; Kavitha, D., Removal of congo red from water by adsorption onto activated carbon preparedfrom coir pith, an agricultural solid waste. *Dyes Pigm.* **2002**, *54*, 47-58. DOI: 10.1016/S0143-7208(02)00025-6.

[100] Tam, N. T.; Liu, Y.; Bashir, H.; Yin, Z.; He, Y.; Zhou, X., Efficient removal of diclofenac from aqueous solution by potassium ferrate-activated porous graphitic biochar: Ambient condition influences and adsorption mechanism. *Int. J. Environ. Res. Public Health.* **2020**, *17*, *291*. DOI: 10.3390/ijerph17010291.

[101] Li, S.; Zhang, X.; Huang, Y., Zeolitic imidazolate framework-8 derived nanoporous carbon as an effective and recyclable adsorbent for removal of ciprofloxacin antibiotics from water. *J. Hazard. Mater.* **2017**, *321*, 711-719. DOI: 10.1016/j.jhazmat.2016.09.065.

[102] Seo, P. W.; Bhadra, B. N.; Ahmed, I.; Khan, N. A.; Jhung, S. H., Adsorptive removal of pharmaceuticals and personal care products from water with functionalized metal-organic frameworks: Remarkable adsorbents with hydrogen-bonding Abilities. *Sci. Rep.* **2016**, *6*, 34462. DOI: 10.1038/srep34462 (2016).

[103] Bhadra, B. N.; Ahmed, I.; Kim, S.; Jhung, S. H., Adsorptive removal of ibuprofen and diclofenac from water using metal-organic framework-derived porous carbon. *Chem. Eng. J.* **2017**, *314*, 50-58. DOI: 10.1016/j.cej.2016.12.127.

[104] Ayati, A.; Shahrak, M. N.; Tanhaei, B.; Sillanpaa, M., Emerging adsorptive removal of azo dye by metal-organic frameworks. *Chemosphere* **2016**, *160*, 30-44. DOI: 10.1016/j.chemosphere.2016.06.065.

[105] El-Shafey, E. I.; Al-Lawati, H.; Al-Sumri, A. S.,

Ciprofloxacin adsorption from aqueous solution onto chemically prepared carbon from date palm leaflets. *J. Environ. Sci.* **2012**, *24*, 1579-1586 DOI: 10.1016/S1001-0742(11)60949-2.

[106] Tam, N. T.; Liu, Y.; Bashir, H.; Yin, Z.; He, Y.; Zhou, X., Efficient removal of diclofenac from aqueous solution by potassium ferrate-activated porous graphitic biochar: Ambient condition influences and adsorption mechanism. *Int. J. Environ. Res. Public Health*. **2020**, *17*, 291. DOI: 10.3390/ijerph17010291.

[107] Ramanayaka, S.; Vithanage, M.; Sarmah, A.; An, T.; Kim, K.; Ok, Y. S., Performance of metal organic frameworks for the adsorptive removal of potentially toxic elements in a water system: A critical review. *RSC Adv.* **2019**, *9*, 34359. DOI: https://doi.org/10.1039/C9RA06879A.

[108] Kim, K. H.; Szulejko, J. E.; Raza, N.; Kumar, V.; Vikrant, K.; Tsang, D. C. W.; Bolan, N. S.; Ok, Y. S.; Khan, A., Identifying the best materials for the removal of airborne toluene based on performance metrics-A critical review. *J. Clean. Prod*. **2019**, *241*, 118408. DOI: 10.1016/j.jclepro.2019.118408.

[109] Szulejko, J. E.; Kim, K.; Parise, J., Seeking the most powerful and practical real-world sorbents for gaseous benzene as a representative volatile organic compound based on performance metrics, *Separ. Purif. Technol.* **2019**, *212*, 980-985. DOI: https://doi.org/10.1016/j.seppur.2018.11.001.

[110] Hurst, J. J.; Wallace, J. S.; Aga, D. S., Method development for the analysis of ionophore antimicrobials in dairy manure to assess removal within a membrane-based treatment system. *Chemosphere.* **2018**, *197*, 271-279. DOI: 10.1016/j.chemosphere.2018.01.028.

[111] Carabineiro, S. A. C.; Thavorn-Amornsri, T.; Pereira, M. F. R., Comparison between activated carbon, carbon xerogel and carbon nanotubes for the adsorption of the antibiotic ciprofloxacin. *Catal. Today.* **2012**, *186*, 29-34. DOI: https://doi.org/10.1016/j.cattod.2011.08.020.

[112] Li, S.; Zhang, X.; Huang, Y., Zeolitic imidazolate framework-8 derived nanoporous carbon as an effective and recyclable adsorbent for removal of ciprofloxacin antibiotics from water. *J. Hazard. Mater.* **2017**, *321*, 711-719. DOI: 10.1016/j.jhazmat.2016.09.065.

[113] Hasan, Z.; Khan, N. A.; Jhung, S. H., Adsorptive removal of diclofenac sodium from water with Zr-based metal-organic frameworks. *Chem. Eng. J.* **2016**, *284*, 1406-1413. DOI: https://doi.org/10.1016/j.cej.2015.08.087.

[114] Wei, H.; Deng, S.; Huang, Q.; Nie, Y.; Wang, B.; Huang, J.; Yu, G., Regenerable granular carbon nanotubes/alumina hybrid adsorbents for diclofenac sodium and carbamazepine removal from aqueous solution. *Water Res.* **2013**, *47*, 4139-4147. DOI: 10.1016/j.watres.2012.11.062.

[115] Ayash, M.; Elnasr, T.; Soliman, M., Removing iron ions contaminants from groundwater using modified nano-hydroxyapatite by nano manganese oxide. *J. Wat. Res. Prot.* **2017**, *11*, 289-809. DOI: 10.4236/jwarp.2019.116048.